



**You have downloaded a document from
RE-BUS
repository of the University of Silesia in Katowice**

Title: Crystallization of amorphous Co₇₇Si_{11.5}B_{11.5} alloy

Author: R. Nowosielski, A. Zajdel, S. Lesz, Beata Kostrubiec, Zbigniew Stokłosa

Citation style: Nowosielski R., Zajdel A., Lesz S., Kostrubiec Beata, Stokłosa Zbigniew. (2007). Crystallization of amorphous Co₇₇Si_{11.5}B_{11.5} alloy. "Archives of Materials Science and Engineering" (Vol. 28, iss. 3 (2007), s. 141-148).



Uznanie autorstwa - Użycie niekomercyjne - Bez utworów zależnych Polska - Licencja ta zezwala na rozpowszechnianie, przedstawianie i wykonywanie utworu jedynie w celach niekomercyjnych oraz pod warunkiem zachowania go w oryginalnej postaci (nie tworzenia utworów zależnych).



UNIwersYTET ŚLĄSKI
W KATOWICACH



Biblioteka
Uniwersytetu Śląskiego



Ministerstwo Nauki
i Szkolnictwa Wyższego



Crystallization of amorphous $\text{Co}_{77}\text{Si}_{11.5}\text{B}_{11.5}$ alloy

R. Nowosielski ^a, A. Zajdel ^{a,*}, S. Lesz ^a, B. Kostrubiec ^b, Z. Stokłosa ^b

^a Division of Nanocrystalline and Functional Materials and Sustainable Pro-ecological Technologies, Institute of Engineering Materials and Biomaterials, Silesian University of Technology, ul. Konarskiego 18a, 44-100 Gliwice, Poland

^b Institute of Materials Science, Silesian University of Technology, ul. Bankowa 12, 40-007 Katowice, Poland

* Corresponding author: E-mail address: aleksandra.zajdel@polsl.pl

Received 31.03.2006; accepted in revised form 10.02.2007

ABSTRACT

Purpose: The investigation results of crystallization of amorphous $\text{Co}_{77}\text{Si}_{11.5}\text{B}_{11.5}$ alloy in tape form, obtained by melt spinning method during annealing in temperature range 373-873 K with step of 50 K in time 1 h, have been presented in the paper.

Design/methodology/approach: The following experimental techniques were used: X-ray diffraction (XRD), electrical resistivity in situ measurements (four-point probe) static and dynamic measurements of magnetic properties (magnetic balance, fluxmeter, Maxwell-Wien bridge).

Findings: The changes of magnetic properties connected with the structure changes involved by crystallization process have been investigated of amorphous $\text{Co}_{77}\text{Si}_{11.5}\text{B}_{11.5}$ alloy.

Practical implications: Amorphous magnetic materials have been around for some time and their applications can be found in many types of industrial products. They include transformers, motors, and a wide variety of magnetic components in sensors, power electronics, electrical energy control/management systems, telecommunication equipment and pulse power devices.

Originality/value: It has been stated that heat treatment leads to crystallization leads to a significant increase of the initial magnetic permeability.

Keywords: Amorphous materials; Electrical properties and magnetic properties; Heat treatment annealing; X-ray diffraction method

MATERIALS

1. Introduction

The metallic glasses represent a novel dual class of metallic materials characterized by amorphous structure and metallic bond providing them with unique physical and mechanical properties that cannot be found either in pure metals or other amorphous materials [1-5]. It has been shown that is a consequence of their microstructure with absence of long distance order atom arrangement [6,7,9,10]. The amorphous state of matter is, however, structurally and thermodynamically unstable and very

susceptible to partial or complete crystallization during thermal treatment or nonisothermal compacting [8]. Amorphous and nanocrystalline alloys based on iron form one of the most interesting groups of soft magnetic materials. The requirements for the soft magnetic alloys with nonequilibrium structure produced by melt quenching technique involve the design of the proper chemical composition that provides improved levels of the properties, such as a high glassforming ability, good casting properties for the alloy which in turn determine the surface quality and uniformity of the meltspun ribbons, as well as an enhanced

thermal stability of both magnetic properties and amorphous structure [11-14]. A lot of papers have been dedicated to amorphous alloys ferromagnetism comprising the results of investigation of magnetic properties for alloys of different content [14-17]. Generally an amorphous structure is assumed to introduce fluctuations in exchange interactions, which influence magnetic behaviour [9, 12]. Amorphous alloys can be prepared by a number of different techniques, e.g. thermal decomposition, mechanical alloying, melt-spinning. Compared to other techniques, rapid solidification processing can form metastable crystalline, quasicrystalline or glassy phases and an extend solid solubility above the equilibrium limit [18-20]. Amorphous alloys for soft magnetic applications are usually given a stress relief annealing treatment to optimize their magnetic properties for low frequency applications [13, 20-22]. In the intermediate to high frequency range, the magnetic properties of Co-based amorphous alloy ribbons may be further improved by the introduction of a few well separated primary crystals which modify the domain structure and reduce eddy current losses. Crystallization in CoSiB alloys resulted in asymmetrically displaced hysteresis loops, the loop displacement increasing number of discrete ϵ -Co crystals clusters. Based magnetic measurements, differential scanning calorimetry and microstructural observations it was concluded that the shift in the hysteresis loops originates from the presence of ϵ -Co crystals within the bulk, rather than at the ribbon surfaces [13-16,21,23]. The crystallization behavior of metallic glasses has been studied by many researchers. It is interesting because it is connected with the changes involved in physical and chemical properties which determine most applications and they can be found in many types of industrial products [9]. They include transformers, motors and a wide variety of magnetic components in sensors, power electronics, electrical energy control/management systems, telecommunication equipment and pulse power devices [15-17]. The wide range of applications arises from the versatile nature of these materials which can provide fast magnetisation reversal with minimal magnetic losses. In certain cases, alloys can be designed for specific applications. In developing a magnetic material, two extreme cases are of interest from an application point of view: one is a material with as high permeability as possible and the other is a material with the saturation induction B_s as high as possible. [20, 23, 24]. In this paper we present and discuss crystallization kinetics and magnetic properties of Co-based amorphous alloy.

2. Experiments

Experiments were carried out on the $\text{Co}_{77}\text{Si}_{11.5}\text{B}_{11.5}$ amorphous alloy. Tapes obtained by planar-flow casting method were 0.020 mm thickness and 10.0 mm width. The samples of 110 mm long were annealed in argon atmosphere in temperature range from 373÷873 K with step of 50 K. The annealing time was constant and equal to 1 hour.

In order to study the structural changes taking place during structural relaxation and crystallization X-ray diffraction analysis (XRD7 SEIFERT – FPM) using cobalt K_α radiation have been used (Table 1). In order to conduct structural study, the high-resolution transmission electron microscope (HRTEM) JEM-3010 was used.

Magnetic properties were determined by making use of static and dynamic measurements of samples in as quenched state and after annealing in temperature range $T_a = 373\div 873$ K. The magnetic permeability μ_r were measured by Maxwell-Wien bridge at frequency about 1 kHz and magnetic field $= 0.5$ A/m; open coil, demagnetization factor was numerically and experimentally determined. The primary magnetisation curve for the ribbons in as quenched state was examined by system equipped with fluxmeter. From this curve the maximum permeability μ_{max} for amorphous $\text{Co}_{77}\text{Si}_{11.5}\text{B}_{11.5}$ alloy in as quenched state was achieved. The saturation magnetic polarization $J = \mu_0 M$ was measured by magnetic balance. Measurements of saturation magnetic polarization $J = \mu_0 M$ were performed for the samples in as quenched state however initial relative magnetic permeability μ_r was performed for samples in as quenched state as well as after annealing.

Table 1.

The diffractometer's parameters used in XRD method for samples of $\text{Co}_{77}\text{Si}_{11.5}\text{B}_{11.5}$ alloy

Diffractometer's parameters	Diffractometer XRD 7, SEIFERT - FPM firm	
	a	b
Current intensity of X – ray tube	40 mA	40 mA
Voltage of X – ray tube	35 kV	35 kV
The time of counting in one measurement's point	7s	20s
Step between measurement's points	$0.05^\circ\Theta$	$0.01^\circ\Theta$

The kinetic of the crystallization was examined as well as by applying electrical resistivity measurements with continuous heating rate 2, 5 and 10 K/min (so called in situ measurements) [11] as measurements of saturation magnetization as a function of temperature $M(T)$. Curves $M(T)$ were recorded by applying magnetic balance technique and samples in as quenched state were heated with heating rate 5 and 10 K/min. The results were presented as normalized curves $M(T)/M(300\text{ K})$. From this data, the Curie temperatures of the amorphous phase T_C can be determined by applying the condition $dM/dT = \text{minimum}$. The Curie temperature of the examined alloy was determined with the precision of about ± 2 K.

From the electrical resistivity measurements of the investigated alloy the crystallization temperature T_{xl} of the amorphous alloy and the effective activation energy for the crystallization E_c were determined. Kissinger method gives the effective activation energy E_c for the process in $\text{Co}_{77}\text{Si}_{11.5}\text{B}_{11.5}$ alloy, which is written as Eq (1)

$$\ln \frac{V_l}{T_h^2} + \ln \text{const} = -\frac{E_c}{k_B} \cdot \frac{1}{T_h} \quad (1)$$

where: E_c is the effective activation energy for the crystallization processes, V_l is a linear heating rate, T_h is the so – called temperature of an homologous point determined for the heating rate V_n , i.e. temperature which the rate of crystallization process is maximum [21], and k_B is the Boltzman constant.

3. Results and discussion

The examinations of structure performed by X-ray diffraction (XRD) technique and high-resolution transmission electron microscopy (HRTEM) show that in as quenched state the $\text{Co}_{77}\text{Si}_{11.5}\text{B}_{11.5}$ alloy has amorphous structure (Fig. 1, Fig 2a, b). In Fig. 1 the X-ray diffraction pattern of the $\text{Co}_{77}\text{Si}_{11.5}\text{B}_{11.5}$ alloy in as quenched state is presented however Fig 2 a and b shows the microstructure image and the corresponding diffraction pattern obtained for the $\text{Co}_{77}\text{Si}_{11.5}\text{B}_{11.5}$ alloy, respectively.

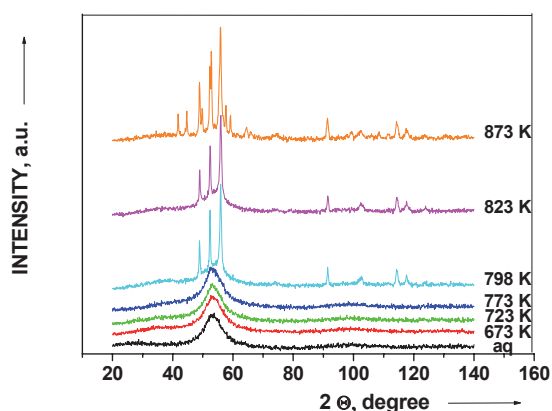


Fig. 1. X-ray diffraction pattern of the $\text{Co}_{77}\text{Si}_{11.5}\text{B}_{11.5}$ alloy in as quenched state and after annealing in temperature range $T_a=673$ -873 K

The investigated $\text{Co}_{77}\text{Si}_{11.5}\text{B}_{11.5}$ alloy in as quenched state has a following magnetic properties: saturation magnetic polarization $J=1.15$ T (Fig. 3), initial relative magnetic permeability $\mu_r=600$ (Fig.4), and maximum permeability $\mu_{max}=4500$ (Fig. 5) (obtained from Fig. 6). The $\text{Co}_{77}\text{Si}_{11.5}\text{B}_{11.5}$ alloy in as quenched state has a high value of resistivity $\rho \cong 1.4 \mu\Omega\text{m}$ (Fig. 4). The obtained physical properties: J , μ_r , μ_{max} and ρ allow to classify the $\text{Co}_{77}\text{Si}_{11.5}\text{B}_{11.5}$ alloy in as quenched state as a soft magnetic material [19].

First stage of crystallization of $\text{Co}_{77}\text{Si}_{11.5}\text{B}_{11.5}$ alloy was found in the temperature range 773 - 823 K (Fig. 1). Fig. 1 shows the XRD data obtained from the $\text{Co}_{77}\text{Si}_{11.5}\text{B}_{11.5}$ alloy ribbons annealing in temperature range from 673 - 773 K can be seen that almost the same structure which in as quenched state.

Increase of the annealing temperature above 773 K leads to changes of structure of the investigated alloy (Fig.1). As can be seen from Fig. 1 at 798 K the crystallization of the amorphous alloy proceeds through nucleation of the hexagonal (h.c.p.) α -Co phase in the amorphous matrix (Table 2). Further increase of the annealing temperature leads to changes in X-ray diffraction pattern (Fig. 1) and at annealing temperature 873 K the existence Co_2B , Co_3B and Co_2Si phases were observed besides to the α -Co phase (Table 2). The results of XRD-method proved that β -Co phase (bcc) did not indicate in the samples of $\text{Co}_{77}\text{Si}_{11.5}\text{B}_{11.5}$ alloy annealed at 873 K for 1 h (see Fig. 7).

Fig. 4 shows as well as resistivity ρ as initial relative magnetic permeability μ_r measured at room temperature plotted

versus 1 h annealing temperature. The resistivity behavior (Fig. 4) is typical for the usual crystallization from the amorphous phase, where the resistivity continuously decreases because the resistivity of the order alloy is lower than disordered one of the some composition [19]. The changes of magnetic properties have been observed with increasing the temperature annealing of investigated alloy. From Fig. 4, it can be recognized that μ_r passes by a distinct maximum (at annealing temperature 723 K) related to formation of nanocrystalline phase α -Co, or annealing out of free volumes (microvoids) formed into during fabrication is observed [23]. The last stage of annealing, in the temperature range from 730 K up to 850 K, is characterized by decrease of magnetic permeability (Fig. 4) of investigated alloy.

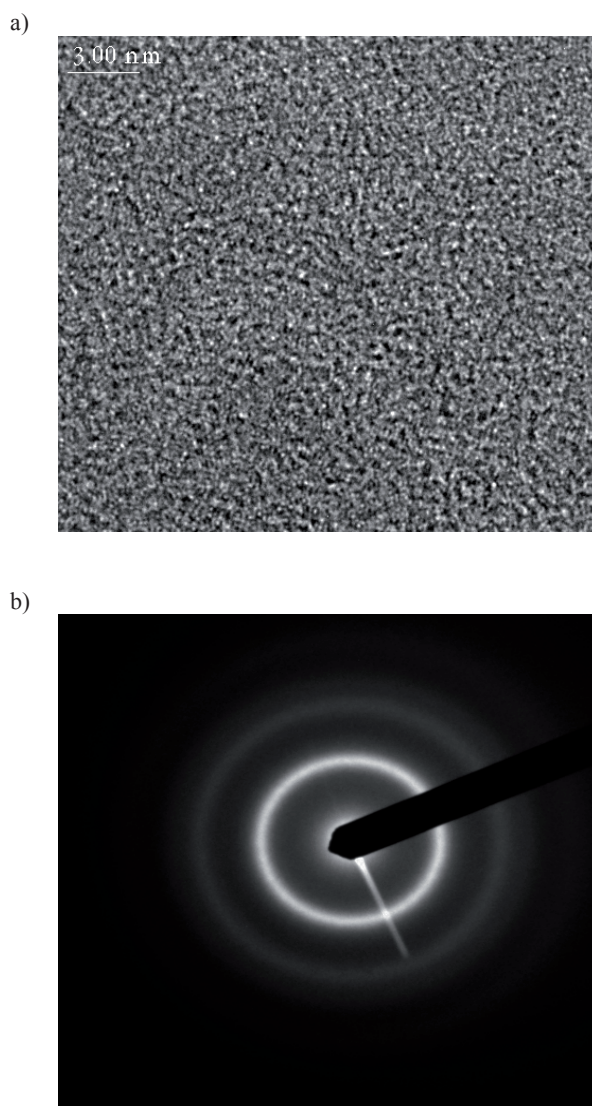


Fig 2. Electron microscopy image (a) and electron diffraction state patterns (b) obtained for $\text{Co}_{77}\text{Si}_{11.5}\text{B}_{11.5}$ alloy in the as quenched

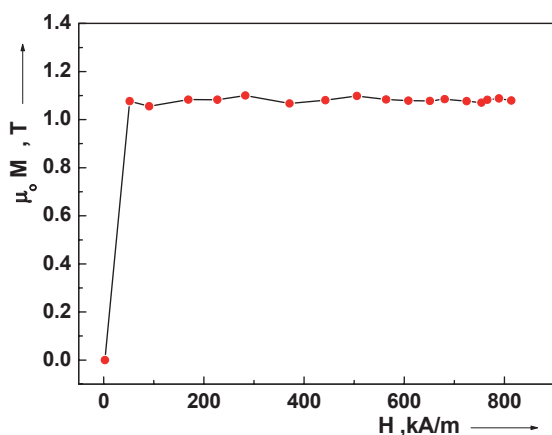


Fig. 3. Saturation magnetic polarization $J=\mu_0 M$ obtained for the $\text{Co}_{77}\text{Si}_{11.5}\text{B}_{11.5}$ alloy in the as quenched state

Existence of borides Co_2B and Co_3B observed (Table 2) leads to decrease of magnetic permeability (Fig. 4). This phenomenon (at temperature above 730 K) can be explained by formation of the equilibrium phases as well as the grain coarsening.

The changes of electrical resistivity of ribbons after linear heating were presented in Fig. 8 to 10. The isochronal resistivity curves determined with the heating rate 2 K/min, 5 K/min and 10 K/min were presented in Fig. 8a, 9a and 10a, respectively. The characteristic temperatures, i.e. first and second stage of crystallization process T_1 and T_2 was determined from the condition $d\rho/dT=0$ (Figs. 8 b, 9 b and 10 b).

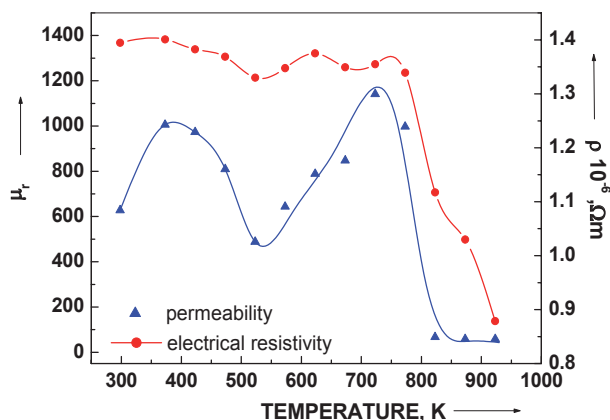


Fig. 4. Initial relative magnetic permeability μ_r and electrical resistivity ρ measured at room temperature for $\text{Co}_{77}\text{Si}_{11.5}\text{B}_{11.5}$ alloy after 1 h annealing.

The temperatures of crystallization depend on the heating rate (Figs. 8 to 10). The observed strong decrease of ρ is due to crystallization of the amorphous alloy. The appearance of a long-range order leads to decrease of ρ value [8].

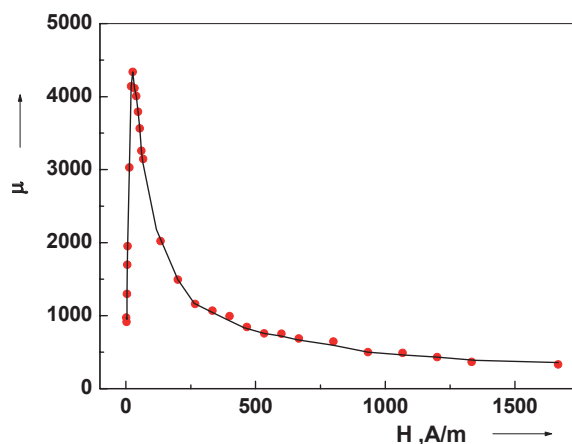


Fig. 5. The maximum permeability μ_{max} achieved from the primary curves of magnetization for $\text{Co}_{77}\text{Si}_{11.5}\text{B}_{11.5}$ alloy in as quenched state

The results achieved from isochronous curves (Fig. 8, 9, 10) in the co-ordinate system $\ln(v/T_h)$ versus T_h^{-1} have been shown in Fig. 11. The effective activation energy E_c of the crystallization process determined from the slope of the straight line (according to equation 1) is 2.2 ± 0.2 eV.

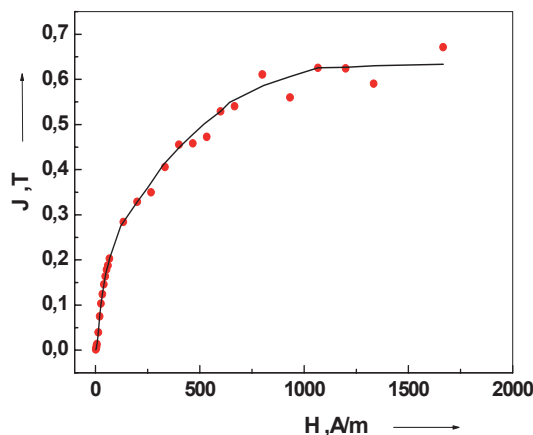


Fig. 6. The primary curve of magnetization (magnetization J versus magnetic field H) for $\text{Co}_{77}\text{Si}_{11.5}\text{B}_{11.5}$ alloy in as quenched state obtained by fluxmeter

Fig. 12a and 13a shows a family of normalized curves $M(T)/M(300\text{ K})$ obtained for $\text{Co}_{77}\text{Si}_{11.5}\text{B}_{11.5}$ alloy with two heating rates: $v=5$ K/min and $v=10$ K/min and the corresponding dM/dT curves (Fig. 12 b and 13 b). As can be seen magnetization of amorphous phase initially decreases in the temperature range from 300 K up to the Curie point. The Curie temperature of the amorphous phase T_c can be determined by applying the condition $dM/dT=\text{minimum}$. The Curie temperature T_c is equal 725 K and 736 K for $v=5$ and 10 K/min, respectively. From the data shown in Fig. 12b and 13b the so-called nanocrystallization temperature T_m (position of the maximum of dM/dT) can be determined.

Table 2.

The phase analysis results for the $\text{Co}_{80}\text{Si}_9\text{B}_{11}$ alloy annealed at $T_a=798$ K, 823 K and 873 K (see Fig. 1)

d,	d _α (hkl) for phases:			
Å	α-Co	Co ₃ B	Co ₂ B	Co ₂ Si
2.500			2.510 (200)	
2.340		2.363 (112)		
2.165*	2.165 (100)			
2.130		2.128 (121)		2.130 (310)
2.100			2.113 (002)	
2.030*	2.023 (002)	2.031 (210)		2.020 (220)
2.000				2.000 (301)
1.980		1.975 (103)	1.983 (211)	1.970 (121)
1.940		1.942 (211)		
1.910*	1.910 (101)			
1.870		1.860 (122)		1.870 (002)
1.850		1.848 (113)		1.850 (311)
1.800			1.815 (112)	
1.740		1.732 (212)		
1.700				1.700 (112)
1.660		1.657 (004)		1.670 (410)
1.616		1.620 (130)	1.616 (202)	
1.590			1.588 (310)	1.600 (130)
1.485	1.480 (102)			
1.250*	1.252 (110)			1.250 (412)
1.187			1.192 (213)	1.190 (113)
1.179			1.183 (330)	
1.167			1.169 (411)	
1.149*	1.149 (103)			
1.105				1.110 (023)
1.101				1.100 (512)
1.083	1.083 (200)			
1.065*	1.066 (112)			
1.046*	1.047 (201)			
1.031				1.032 (332)
1.016*	1.015 (004)			
0.987			0.973 (204)	

d – lattice parameters calculated from Fig. 1

d_α – lattice parameters of identified phases [17]

* - the peak appearing in $\text{Co}_{80}\text{Si}_9\text{B}_{11}$ alloy annealed at $T_a=798$ and 823 K, too

The value of T_m deduced in this way corresponds to the highest formation rate of the new ferromagnetic phase. With increasing heating rate the maxima of dM/dT shift towards higher temperatures which is a characteristic feature of thermally activated (diffusion controlled) process [25].

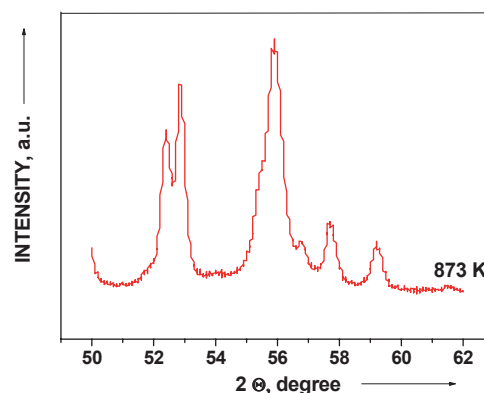


Fig. 7. X – ray diffraction pattern of the $\text{Co}_{77}\text{Si}_{11.5}\text{B}_{11.5}$ alloy after annealing at temperature 798 K for 1 h. The parameters of diffractometer – see Table 1

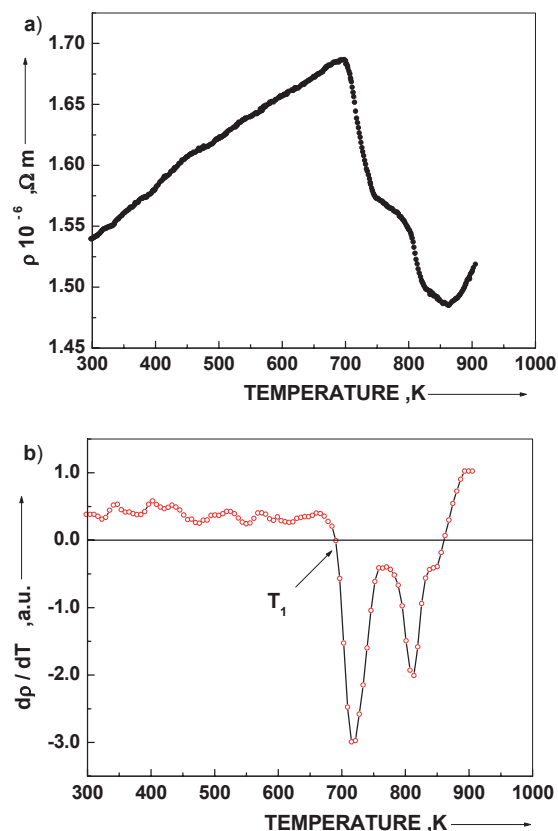


Fig. 8. (a) The electrical resistivity curves for $\text{Co}_{77}\text{Si}_{11.5}\text{B}_{11.5}$ alloy obtained with heating rate 2 K/min (b) The $d\rho/dT$ curve for data presented in (a)

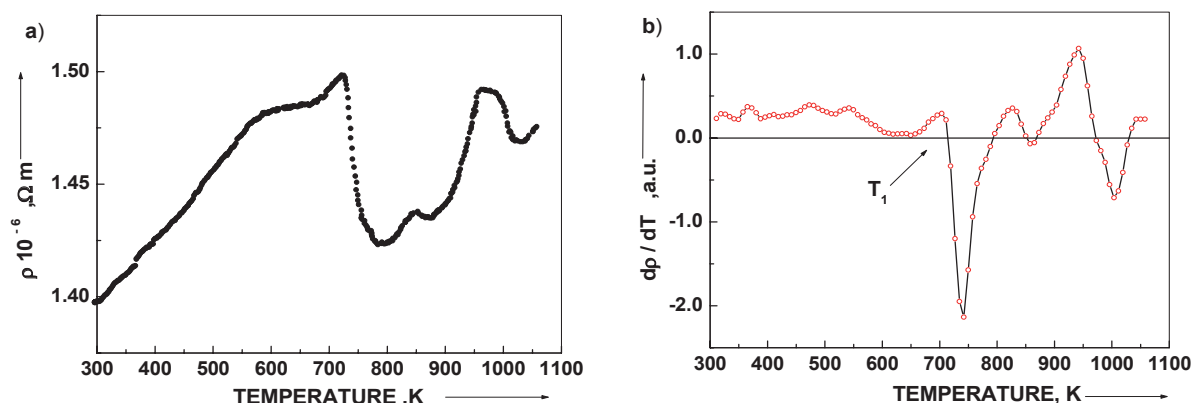


Fig. 9. (a) The electrical resistivity curves for $\text{Co}_{77}\text{Si}_{11.5}\text{B}_{11.5}$ alloy obtained with heating rate 5 K/min (b) The dp/dT curve for data presented in (a)

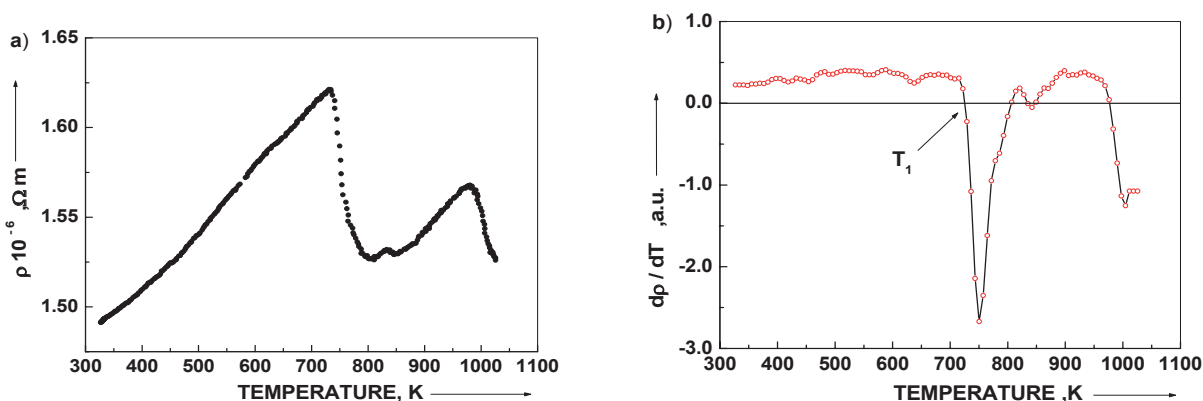


Fig. 10. (a) The electrical resistivity curves for $\text{Co}_{77}\text{Si}_{11.5}\text{B}_{11.5}$ alloy obtained with heating rate 10 K/min (b) The dp/dT curve for data presented in (a)

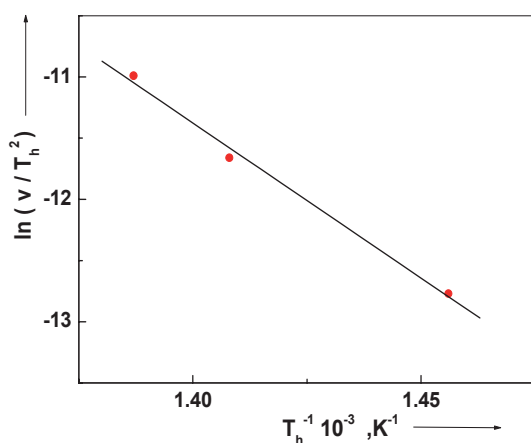


Fig. 11. Plot of $\ln(v/T_h^2)$ versus T_h^{-1} for $\text{Co}_{77}\text{Si}_{11.5}\text{B}_{11.5}$ alloy

4. Conclusions

The worked out investigations have been showed that heat treatment of amorphous $\text{Co}_{77}\text{Si}_{11.5}\text{B}_{11.5}$ alloy in temperature range 373÷873 K involves two-stages crystallization and leads to radical changes of magnetic properties of tapes.

The $\text{Co}_{77}\text{Si}_{11.5}\text{B}_{11.5}$ alloy ribbons annealing in temperature range from 673-773 K can be seen that almost the same structure which in as quenched state. First stage of crystallization of $\text{Co}_{77}\text{Si}_{11.5}\text{B}_{11.5}$ alloy was found in the temperature range 773-823 K. The crystallization process leads to increase of initial relative permeability from 600 for ribbons in as quenched state to 1200 for ribbons heat treated at temperature 723 K. This phenomenon is connecting with the formation of the hexagonal α -Co phase in an amorphous matrix at the temperature $T=798$ K and this is the first stage of the crystallization process. In the temperature $T = 873$ K appearance of boride phase Co_2B , Co_3B and silicide phase Co_2Si was state. It is the second stage of crystallization. The existence of boride phases was confirmed by a decrease of initial magnetic permeability μ_r after annealing in the temperature range from 730 K up to 873 K. The secondary crystallization is known to cause grain coarsening of phases and the degradation of the soft magnetic properties [23].

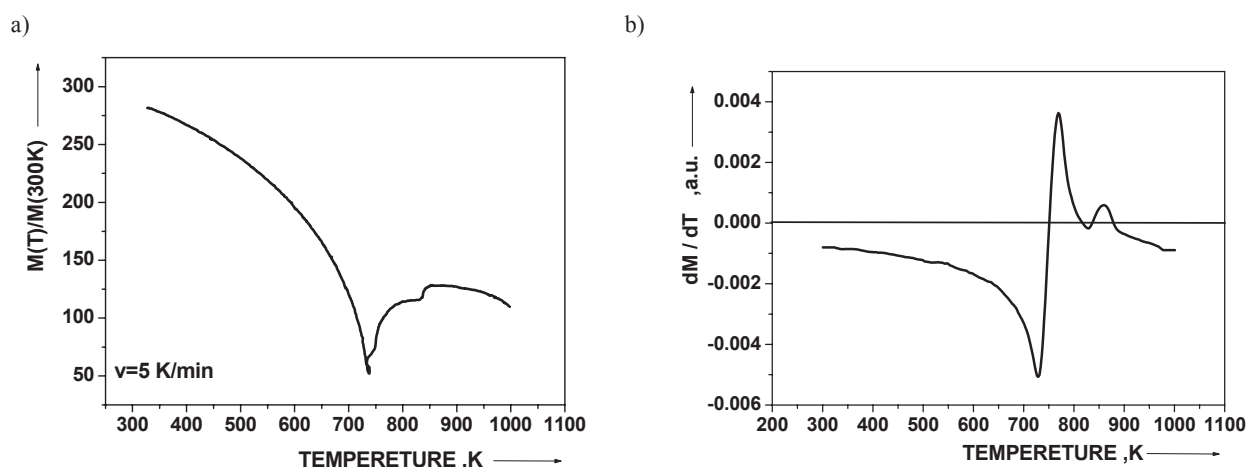


Fig. 12. (a) Normalized magnetization versus temperature T of $\text{Co}_{77}\text{Si}_{11.5}\text{B}_{11.5}$ alloy (b) dM/dT curves for the data presented in (a)

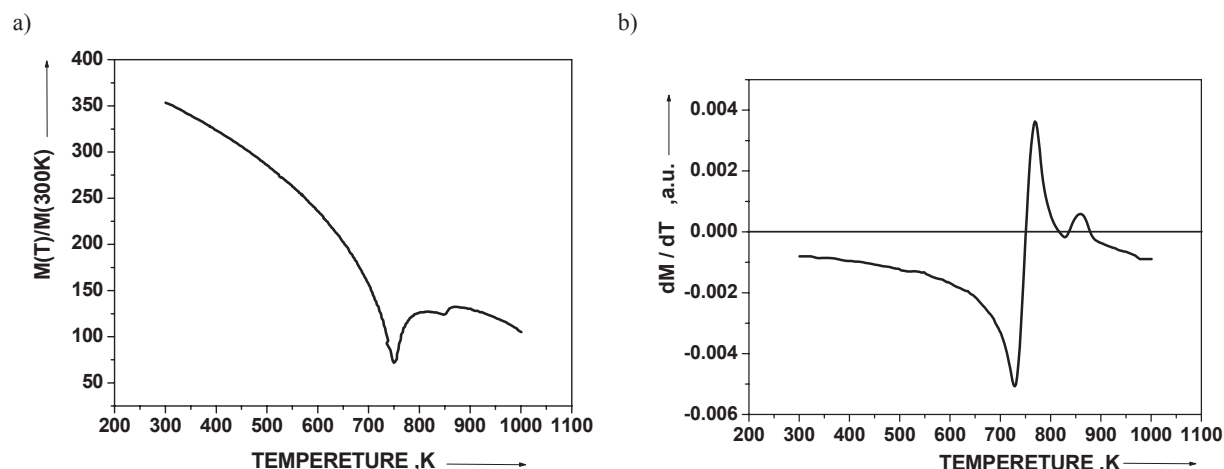


Fig. 13. (a) Normalized magnetization versus temperature T of $\text{Co}_{77}\text{Si}_{11.5}\text{B}_{11.5}$ alloy (b) dM/dT curves for the data presented in (a)

Additional information

The presentation connected with the subject matter of the paper was presented by the authors during the 14th International Scientific Conference on Achievements in Mechanical and Materials Engineering AMME'2006 in Gliwice-Wisła, Poland on 4th-8th June 2006

References

- [1] A. Kalezic-Glisovic, L. Novakovic, A. Maricić, D. Minic, N. Mitrović, Investigation of structural relaxation, crystallization process and magnetic properties of the Fe-No-Si-B-C amorphous alloy, *Materials Science and Engineering B* 131 (2006) 45-48.
- [2] D.S Jong, J.H. Kim, E. Fleury, W.T Kim, Synthesis of ferromagnetic Fe-based bulk glassy alloys in the Fe-Nb-B-Y system, *Journal Alloys Compounds* 389 (2005) 159-164.
- [3] G. Buttino, A. Cecchetti, M. Poppi, Temperature dependence of structural and magnetic, relaxation in amorphous and nanocrystalline Co-based alloy, *Journal of Magnetic and Magnetism Materials* 241 (2002) 183-189.
- [4] M.F. Ashby, A.L.Greer, Metallic glasses as a structural materials, *Scripta Materialia* 54 (2006) 321-326.
- [5] K.G Raval, K.N. Lad, A. Pratap, A.M. Awashi, S. Bhardwaj, Crystallization kinetics of a multicomponent Fe-based amorphous alloy using modulated differential scanning calorimetry, *Tchermochim Acta* 425 (2005) 47.
- [6] P. Gramatyka, R. Nowosielski, P. Sakiewicz, Magnetic properties of polymer bonded nanocrystalline polder, *Journal of Achievements in Materials and Manufacturing Engineering* 20 (2007) 115-118.

- [7] B. Ziębowicz, D. Szewieczek, L.A. Dobrzański, New possibilities of application of composite materials with soft magnetic properties, *Journal of Achievements in Materials and Manufacturing Engineering* 20 (2007) 207-210.
- [8] J. Konieczny, L.A. Dobrzański, A. Przybył, J. Wysłocki, Structure and magnetic properties of powder soft magnetic materials, *Journal of Achievements in Materials and Manufacturing Engineering* 20 (2007) 139-142.
- [9] R. Nowosielski, A. Zajdel, S. Lesz, B. Kostrubiec, Z. Stokłosa, Crystallization kinetics of an amorphous $\text{Co}_{77}\text{Si}_{11.5}\text{B}_{11.5}$ alloy, *Journal of Achievements in Materials and Manufacturing Engineering* 17 (2006) 183-189.
- [10] D. Szewieczek, J. Tyrlik-Held, S. Lesz, Changes of mechanical properties and fracture morphology of amorphous tapes involved by heat treatment, *Journal of Materials Processing Technology* 109 (2001) 190-195.
- [11] D. Szewieczek, J. Tyrlik-Held, S. Lesz, Proceedings of the Scientific Conference „Materials, Mechanical and Manufacturing Engineering” M³E’2000, Gliwice, 2000, 267-272.
- [12] P. Kwapuliński, J. Rasek, Z. Stokłosa, G. Haneczok, Magnetic properties of amorphous and nanocrystalline alloys based on iron, *Journal of Materials Processing Technology* 157-158 (2004) 735- 742.
- [13] R. Hasegawa, Advances in amorphous and nanocrystalline magnetic materials, *Journal of Magnetism and Magnetic materials* 304 (2006) 187-191.
- [14] R. Hasegawa, Present status of amorphous soft magnetic alloys, *Journal of Magnetism and Magnetic Materials* 240 (2000) 215-216.
- [15] Z. Stokłosa, J. Rasek, P. Kwapuliński, G. Haneczok, G. Bzdura, J. Lełątko, Optimization of soft magnetic properties in nanoperm type alloys, *Material Science and Engineering C* 23 (2003) 49-53.
- [16] L.A. Dobrzański, R. Nowosielski, J. Konieczny, A. Przybył, Soft magnetic nanocomposite with powdered metallic ribbon based on cobalt and polymer matrix, *Journal of Materials Processing Technology* 162-163 (2005) 20-28.
- [17] S. Lesz, R. Nowosielski, A. Zajdel, B. Kostrubiec, Z. Stokłosa, Structure and magnetic properties of the amorphous $\text{Co}_{80}\text{Si}_9\text{B}_{11}$ alloy, *Journal of Achievements in Materials and Manufacturing Engineering* 18 (2006) 155-158.
- [18] R. Nowosielski, A. Zajdel, A. Baron S. Lesz, Influence of crystallization on amorphous $\text{Co}_{77}\text{Si}_{11.5}\text{B}_{11.5}$ alloy on corrosion behavior, *Journal of Achievements in Materials and Manufacturing Engineering* 20 (2007) 167-170.
- [19] S. Lesz, R. Nowosielski, Z. Stokłosa, B. Górka Kostrubiec, Proceedings of the 11th International Scientific Conference on „Contemporary Achievements in Mechanics, Manufacturing and Materials Science” CAM3S’2005, Gliwice-Zakopane, 2005, 574-577.
- [20] T.Y. Byun, Y. Oh, C.S. Yoon, C.K. Kim, Crystallization and magnetic properties of $(\text{Co}_{0.75}\text{Cr}_{0.25})_{80}\text{Si}_5\text{B}_{15}$ metallic glass, *Journal of Alloys and Compounds* 368 (2004) 283-286.
- [21] J. Rasek, Some diffusion phenomena in crystalline and amorphous metals, Silesian University Press, Katowice (2000), (in Polish).
- [22] V. Stelmukh, A. Gurov, L. Voropaeva, N. Novokhatskaya, A. Serebryakov, Nanocrystallization of amorphous Co-Si-B alloys with strong compound forming additions, *Journal of Non – Crystalline Solids* 192-193 (1995) 570-573.
- [23] Z. Stokłosa, J. Rasek, P. Kwapuliński, G. Haneczok, G. Bzdura, J. Lełątko, Optimization of soft magnetic properties in nanoperm type alloys, *Material Science and Engineering C* 23 (2003) 49-53.
- [24] R. Jenkins, W.F. McClune, T.M. Maguire, et al., Powder Diffraction Data, JCPDS – International Centre for Diffraction Data, 1601 Parklane, Swarthmore, PA 19081, USA, 1986.
- [25] A. Chrobak, D. Chrobak, G. Haneczok, P. Kwapuliński, Z. Kwolek, M. Karolus, Influence of Nb on the first stage of crystallization in $\text{Fe}_{86-x}\text{Nb}_x\text{B}_{14}$ amorphous alloys, *Materials Science and Engineering A* 382 (2004) 401-406.